Nuclear Engineering and Design 423 (2024) 113211

Contents lists available at ScienceDirect

Nuclear Engineering and Design

journal homepage: www.elsevier.com/locate/nucengdes

Fragmentation of fuel particles in rolling U_3Si_2-Al dispersion fuel plates

Michelangelo Durazzo [a,*], Gilberto Hage Marcondes [a], Elita Fontenele Urano de Carvalho [a], Guilherme Duarte de Barros [b], Ricardo Mendes Leal Neto [a]

[a] Nuclear and Energy Research Institute, IPEN-CNEN/SP, São Paulo, Brazil
[b] Anhembi Morumbi University, São Paulo, Brazil

ARTICLE INFO

Keywords:
Dispersion fuel
Fuel plate
U_3Si_2-Al
Fragmentation
Rolling
Fuel fabrication
Research reactors

ABSTRACT

The Nuclear and Energy Research Institute (IPEN-CNEN/SP) has recently developed a process to produce the nuclear fuel required to run the Brazilian Multipurpose Reactor (RMB), using U_3Si_2-Al dispersion in plate-type fuel elements. Since the late 1980s, regular production of dispersion-based fuel plates has kept the maximum fines content (<44 μm) of 20 wt%. However, IPEN's U_3Si_2 powder manufacturing process typically generates fines between 25 and 30 wt%, making it necessary to discard and recycle about 5 to 10 wt% of the powder during manufacturing. The severe fines requirements necessitate careful comminution with multiple intermediate screening steps, which has a negative impact on RMB's fuel production scalability (60 elements per year). To improve the current fines content specification for the powder, this study focuses on looking into U_3Si_2 particle fragmentation during fuel plate manufacturing. Quantitative microscopy methods and image analysis were employed. The findings revealed a significant increase in fines content during the rolling process, with levels reaching up to 59 wt%. Hence, to ensure high-quality dispersion, it becomes crucial to specify the fines content in the fuel plate obtained after rolling rather than just in the original powder. The results recommend that a new U_3Si_2 powder specification could allow a maximum fine content of 30 wt%. More research is ongoing to confirm this recommendation.

1. Introduction

The preparation of powders for fabricating dispersion fuel elements is one of the most expensive and crucial steps in the process. It requires a high yield of fuel particles within the required range of size, dispersed in an aluminum matrix. The size range is imposed by fission fragments that cause damages in the matrix (Weber and Hirsch, 1955; Weber and Hirsch, 1956; White et al., 1957; Weber, 1959). The choice of particle size is often a trade-off between using larger particles to achieve a good dispersion quality and minimizing processing costs by reducing the formation of fine particles (<44 μm).

Since the 1990s, there has been a noticeable scarcity of literature that provides specific details regarding the content of particles smaller than 44 μm (referred to as "fines") used in the manufacturing of U_3Si_2-Al dispersion fuel. Manufacturers often consider the fines content as "proprietary data" and do not disclose it openly. However, it is evident that a prevailing trend among most manufacturers is to limit the fines content to 25 wt%. Nevertheless, there are some exceptions to this trend. CERCA, for instance, appears to use 40 wt% (or potentially even higher) fines in their dispersion fuel. BATAN (the National Nuclear Energy Agency of Indonesia) employs a fines content of 29 wt% in their U_3Si_2-Al fuel (Suripto et al., 1995). Argentina, as reported by Adelfang et al. (2002), utilizes an average fines content of 38 wt%. FMPP (Egyptian Fuel Manufacturing Pilot Plant) pushes the limit further by using up to 50 wt% (U_3O_8) fines (Abdelrazek et al., 1999). Consequently, the fines content in U_3Si_2-Al dispersion fuel varies across different manufacturers, with these exceptions deviating from the typical 25 wt% limit.

The Nuclear and Energy Research Institute (IPEN-CNEN/SP) has established a routine production process for manufacturing the nuclear fuel required to operate its research reactor, IEA-R1. Since 2007, the institute has been engaged in the production of fuel plates utilizing U_3Si_2-Al dispersion technology (using LEU – Low Enriched Uranium – 20 wt% U-235). To date, a total of 1389 plates, encompassing 74 fuel elements, have been successfully manufactured, each boasting a uranium loading of 3.0 gU/cm^3. The U_3Si_2-Al fuel elements have proven to be effective, as evidenced by their good performance during a seven-year irradiation period. These fuel elements have achieved a burn-up of 50 % without experiencing any significant issues. IPEN-CNEN/SP is

* Corresponding author at: Av. Prof. Lineu Prestes, 2242, Cidade Universitária, CEP 05508-000 São Paulo, SP, Brazil.
E-mail address: mdurazzo@ipen.br (M. Durazzo).

https://doi.org/10.1016/j.nucengdes.2024.113211
Received 27 November 2023; Received in revised form 14 March 2024; Accepted 10 April 2024
Available online 17 April 2024

presently engaged in the preparation for the fabrication of fuel elements requisite for the operation of a forthcoming research reactor intended for construction in Brazil. The reactor is envisaged to be a 30 MW open pool-type facility utilizing low enriched uranium (LEU) fuel. The features of the novel research reactor, denominated as the Brazilian Multipurpose Reactor (RMB), are delineated by Perrotta and Soares (2014).

The fuel elements manufactured at IPEN-CNEN/SP are of the MTR (Materials Testing Reactor) type (Cunningham and Boyle, 1955). The production of dispersion-based fuel plates started in the late 1980s, utilizing U_3O_8-Al dispersion with a uranium load of 2.3 gU/cm^3. During this period, a maximum fines content of 20 wt% was established, drawing from irradiation test outcomes conducted in the Oak Ridge Research Reactor (ORR). It was observed that the majority of manufacturers adhered to fines content ranging from 17-18 wt% (Copeland et al., 1987). This limitation on fines content has persisted to the present day, even after the introduction of U_3Si_2-Al fuel.

IPEN's U_3Si_2 powder manufacturing process typically yields particles smaller than 44 μm in the range of 25 to 30 wt%. Consequently, approximately 5 to 10 wt% of the powder produced must be discarded and recycled during manufacturing. Moreover, due to the existing constraint of limiting fines to 20 wt%, meticulous comminution with multiple intermediate sieving operations between crushing is required. This circumstance has prompted IPEN-CNEN/SP to place more attention to its specification regarding the fines content, in the sense of increasing the currently specified value.

It is important to acknowledge that due to the inherent brittleness of U_3Si_2, a considerable number of fuel particles tend to fracture during the rolling process, leading to an effective increase in the quantity of fines compared to the original powder. The fragmentation of U_3Si_2 particles has been qualitatively observed in previous studies through the analysis of the microstructural evolution of fuel plate meat (Durazzo et al., 2017a).

The primary objective of this study is to investigate the fragmentation of U_3Si_2 particles during the rolling process used to produce dispersion fuel plates. The research presents findings related to the determination of fines concentration (particles smaller than 44 μm) at different stages of the rolling process. An evaluation of the fragmentation properties of U_3Si_2 dispersed in aluminum can provide data to inform discussions on the limitation of fines in the powder. Initially, the U_3Si_2 powder contained 20 wt% fines, but this value increased to 59 wt % in the fuel plate meat after the fabrication of the plates. The maximum particle size experienced a reduction during the fabrication process, decreasing from 150 μm to about 100 μm. The results reveal that it is more crucial to specify the fines content in the fuel plate meat after the manufacturing process, rather than in the starting powder.

2. Experimental

The technique of manufacturing fuel plates through a sequence of hot and cold rolling is widely employed in the production of fuel elements for research reactors worldwide. This well-established method involves the assembly of multiple fuel plates with adequate spacing to facilitate the flow of water, serving as both a coolant and a moderator. These fuel plates consist of a meat containing fissile material, completely enveloped by a protective aluminum cladding (Weber and Hirsch, 1955). The fabrication of fuel plates employs a well-known technique known as the "picture frame technique." This method entails placing the fuel meat within an aluminum frame and enclosing it with aluminum plates, which are subsequently rolled together to form a cohesive structure. A visual representation of this plate fabrication technique can be observed in Fig. 1 (Durazzo and Riella, 2015; Kaufman, 1962). The fuel plates utilized in the current study were manufactured using this plate fabrication technique.

Powder metallurgy techniques were employed in the production of the fuel meats, also referred to as "briquettes," using natural U_3Si_2 as the uranium composite. These briquettes were fabricated by combining powdered U_3Si_2 with pure aluminum powder, which served as the structural matrix material. Scanning electron micrographs (Fig. 2) show the characteristic appearance of U_3Si_2 particles (A) and aluminum particles (B). The briquettes were rectangular parallelepipeds with rounded

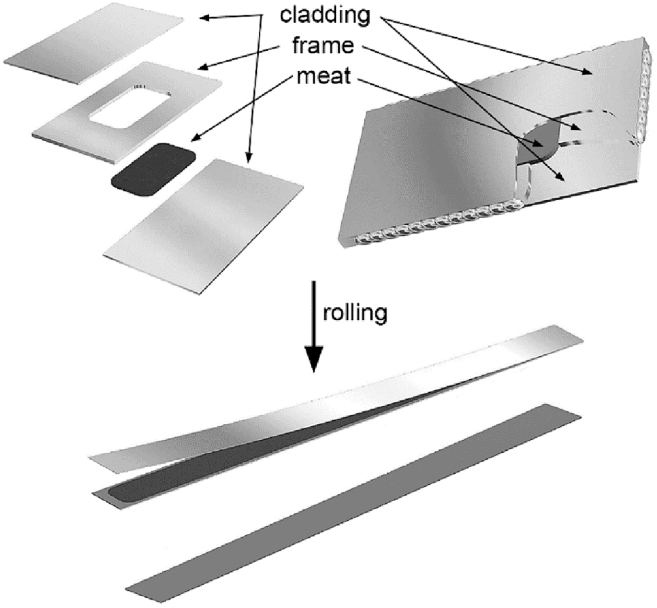

Fig. 1. Picture frame technique used to manufacture fuel plates.

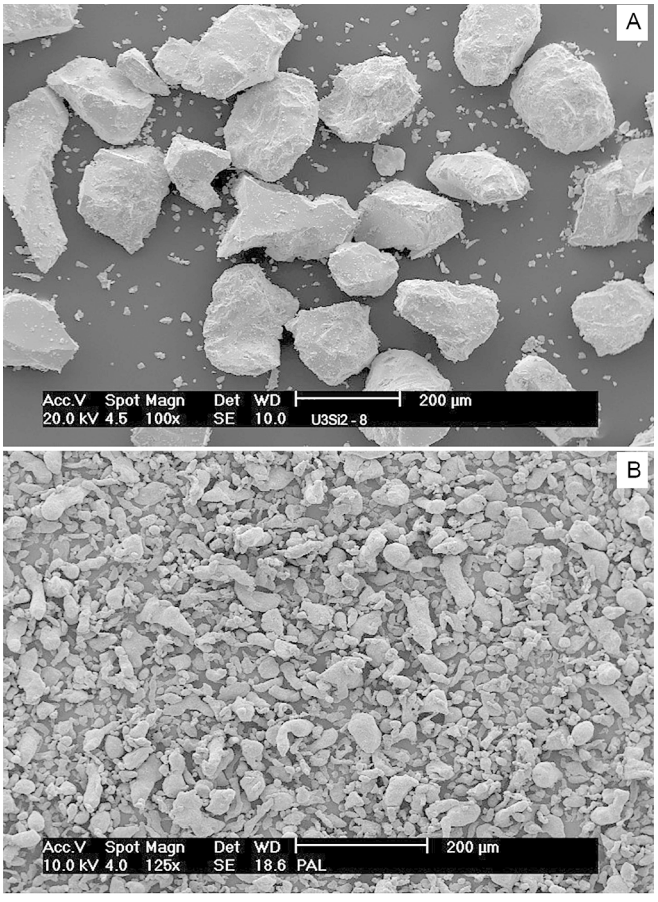

Fig. 2. Scanning electron micrographs (secondary electron images) illustrating the characteristic morphology of U_3Si_2 (A) and aluminum (B) powders.

corners. To prepare each individual briquette, the powders were weighed separately and then blended together. The pressing operation was performed using a double-effect hydraulic press, applying a pressing pressure of 500 MPa to all briquettes. The briquettes had a thickness of 4.2 mm.

The intermetallic U_3Si_2 was produced using an induction furnace from uranium metal (92.5 wt%) and metallic silicon (7.5 wt%), molten inside a zirconia crucible. Details on uranium metal production at IPEN-CNEN/SP are available in previous work (Durazzo et al., 2017b). A 15 kW induction furnace was utilized for the process. The furnace was placed under a vacuum of 0.13 Pa and flushed with an argon atmosphere. The blend was melted inside a zirconia crucible within the induction furnace, reaching a temperature of 1800 °C. This specific intermetallic compound requires such high temperature for adequate homogenization prior to solidification. The temperature was maintained at 1800 °C for 1 min to ensure compositional homogeneity before casting into a copper ingot mold. An optical pyrometer was used to measure the temperature accurately.

To produce powder, the U_3Si_2 ingot was transferred to an argon-filled glove box. Within the glove box, the ingot underwent crushing and milling processes. The initial crushing was carried out manually using a hardened steel mortar, yielding granules smaller than 4 mm. Several intermediate sieving operations were performed to control the generation of fines. The sieve set consisted of a coarse sieve with a 4 mm opening, a sieve with a 150 μm opening, a fine sieve with a 44 μm opening, and a catch compartment. The material was sieved to classify it into size ranges: greater than 4 mm, between 4 mm and 150 μm, and less than 44 μm. The fractions were stored separately. Granules larger than 4 mm were manually crushed once more. The separated fractions smaller than 150 μm are now suitable as fissile particles in the dispersion fuel.

After the initial crushing, the granules ranging in size from 4 mm to 150 μm were collected for the final grinding stage. The final grinding process was carried out meticulously, with intermediate sieving, to minimize the generation of fines. The fraction between 4 mm and 150 μm underwent grinding and subsequent sieving to produce U_3Si_2 powder with a size smaller than 150 μm. The sieving operation was performed using a set of two sieves to separate the fractions with sizes between 150 μm and 44 μm, as well as those smaller than 44 μm (fines). These fractions were stored separately for further use.

The fines content was adjusted to 20 wt% by carefully weighing the fraction between 150–44 μm and precisely determining the mass required to achieve the desired percentage of fines, with an accuracy of 0.01 g. Subsequently, the powders were blended for 1 h using a Turbula T2F mixer to ensure uniformity throughout the batch. A typical U_3Si_2 powder batch consisted of 3 kg and has a density of 12.00 g/cm^3, as determined by helium pycnometry. However, it is worth noting that the typical fines content produced ranged from 25 to 30 wt%. Any fines exceeding the target of 20 wt% were recovered and reintroduced into the process in the form of UF_4.

In this study, the fuel plate was manufactured with the same uranium loading as the U_3Si_2-Al fuel currently produced at IPEN-CNEN/SP, which corresponds to a uranium loading of 3.0 gU/cm^3. As a result, the dispersion contained a volume fraction of 27 % U_3Si_2 (Durazzo et al., 2007).

The fuel plates are designed to have final nominal dimensions of 625 mm in length, 71 mm in width, and 1.52 mm in thickness. The fuel meat is specified to have nominal dimensions of 600 mm in length, 65 mm in width, and 0.76 mm in thickness. For the frame plate, a thickness of 4.2 mm was used, while the cover plates had a thickness of 2.5 mm. The width and length of the frame and cover plates were chosen to ensure sufficient material surrounding the briquette, fulfilling the structural requirements of the frame. In this case, the dimensions used for the frame and cover plates were 200 mm in length and 120 mm in width. The material employed for both the frame and covers was 6061 aluminum.

The assembly, comprising the frame, briquette, and two cover plates, was rolled to achieve the required dimensions and ensure complete sealing of the fuel. The briquette and frame were bonded to the covers during the hot-rolling process. To ensure optimal bonding quality, the frames and covers were carefully wiped with acetone and then etched with a 10 wt% sodium hydroxide solution and 40 % nitric acid. The assembly was then TIG welded, leaving approximately 10 mm from each corner unwelded to facilitate the release of any trapped air during the initial hot rolling passes. For more comprehensive details on the preparation of the assembly for rolling, please refer to the previous work by Durazzo et al., (2017a).

2.1. Sample fabrication

The assemblies underwent a hot-rolling process to transform them into plates and create a strong bond between the cover plates, frames, and briquettes. Prior to hot rolling, the assemblies were preheated for 1 h in an electric furnace equipped with a hot-air circulation blower. The hot rolling temperature was set at 450 °C. Between each rolling pass, the assemblies were reheated for 15 min. Table 1 presents the rolling schedule employed at IPEN-CNEN/SP for the production of fuel plates, providing an overview of the sequence of rolling passes. To monitor the thickness of the hot-rolled plates, a tungsten-carbide-tipped micrometer was employed after each pass. The cold-rolling process was conducted using a high precision mill, employing two rolling passes. The mill's accuracy, with a precision of approximately 0.02 mm, ensured the desired thickness of the cold-rolled plates. Comprehensive information regarding the rolling process can be found in prior research studies (Durazzo et al., 2017a).

This work utilized the conventional rolling scheme employed in the routine fabrication of fuel plates, as outlined in Table 1. The process involved nine hot rolling passes followed by two cold rolling passes, resulting in a thickness reduction of 83.6 %.

To capture the unique deformation stage of the fuel assembly during the rolling process, a fuel plate was extracted after each rolling pass. This created a sample that accurately represented the condition of a fuel plate at that specific stage of rolling. Additionally, a briquette that had been pressed but not rolled was examined, providing microstructural insights into the initial fuel meat. Table 2 presents the sampling scheme used in this study.

Following each rolling pass, the fuel plate was sampled. Rectangular sections measuring approximately 10 mm in width and 15 mm in length were cut from four distinct positions: two specimens from the end regions of the fuel meat and two specimens from the central region, all aligned with the rolling direction. Each sample was carefully identified and embedded in acrylic resin. After each rolling pass, the U_3Si_2 particle size distribution was examined using quantitative metallography techniques. In addition, U_3Si_2 powder and an undeformed briquette was

Table 1
Rolling scheme traditionally adopted at IPEN-CNEN/SP for the production of fuel plates.

Pass	Reduction (%)	Gage (mm)	Heating Time (min)
0	0	9.20	preheating (60 min)
Hot Rolling			
1	25	6.93	15
2	25	5.20	15
3	15	4.42	15
4	15	3.76	15
5	15	3.20	15
6	15	2.72	15
7	15	2.31	15
8	13	2.01	15
9	13	1.75	blistering test (60 min)
Cold Rolling			
10	7	1.63	no heating
11	7	1.52	no heating
final		1.51	final adjustment

Table 2
Sampling scheme for following the U_3Si_2 particle size evolution during fuel plate fabrication.

Rolling Pass	Thickness of Picture-Frame Assembly (mm)										
	P1	P2	P3	P4	P5	P6	P7	P8	P9	P10	P11
	hot-rolling										
Briquette	→ withdrawn for analysis (WA)										
P1	6.91	→	WA								
P2	6.93	5.21	→	WA							
P3	6.90	5.19	4.40	→	WA						
P4	6.96	5.23	4.43	3.78	→	WA					
P5	7.00	5.25	4.46	3.80	3.23	→	WA				
P6	6.90	5.20	4.42	3.77	3.20	2.75	→	WA			
P7	7.05	5.26	4.48	3.80	3.24	2.77	2.33	→	WA		
P8	7.10	5.27	4.48	3.82	3.26	2.78	2.33	2.00	→	WA	
P9	6.95	5.22	4.43	3.76	3.21	2.72	2.30	2.01	1.75	→	WA
	cold-rolling										
P10	6.93	5.22	4.41	3.77	3.21	2.73	2.32	2.02	1.76	1.63	→ WA
P11	6.97	5.23	4.44	3.78	3.23	2.75	2.33	2.02	1.75	1.64	1.53 → WA

prepared for quantitative metallography as well. All the samples underwent grinding and polishing processes as part of the preparation procedure.

The longitudinal section of the samples, aligned with the rolling direction, was chosen to observe the phenomenon known as "stringering," which involves the fragmentation of particles followed by the alignment of the fragments. Examining the cross-section of the sample cut in the longitudinal direction allowed us to observe the maximum degree of fragmentation in the U_3Si_2 particles. This is evident in the scanning electron micrographs presented in Fig. 3. Fig. 3A shows fragmented U_3Si_2 particles being entrained by the flow of the aluminum matrix during the rolling deformation. Small particles are transported by the flow of aluminum surrounding larger particles. The phenomenon known as "stringering" is also clearly evident. In Fig. 3B, it can be observed that the flow of aluminum, which carries small particles, encounters hindrance from two large particles, resulting in the entrapment of several particles. However, some smaller particles successfully bypass the larger particles by being carried along with the aluminum flow. Additionally, the phenomenon of stringering is clearly visible in the image. Fig. 3 also provides an illustration of the typical image utilized in this study to measure the sizes of U_3Si_2 particles.

2.2. U_3Si_2 particle size measurement

The polished sections of the samples were observed using a Thermo Scientific Prisma E scanning electron microscope (SEM). The obtained images were subjected to analysis using the public domain program ImageJ, which enabled the measurement of the particle areas in 2-D polished sections. As an example of image processing, Fig. 4A displays the original image captured from a sample taken from rolling pass 4, while Fig. 4B exhibits the processed image. The noise below 3 μm was eliminated, and the filter Watershed was employed to separate interconnected particles. Superficial imperfections on the particle surface that do not qualify as cracks dividing it into fragments were eliminated. Additionally, boundary objects were removed from the image to avoid measuring the particles at image borders.

The particle size of U_3Si_2 (equivalent diameter) obtained from the polished sections were converted into volumetric size distributions using the Saltikov method (Saltikov, 1967), assuming spherical shape particles. This transformation was done to obtain volumetric distributions that could be directly compared with the particle size distributions determined through sieving. The mass fraction of particles with a diameter less than 44 μm (fines) was determined from the cumulative diameter curve using linear interpolation between Saltikov classes. This determination was further confirmed graphically, as depicted in Fig. 5.

A zoom feature was utilized during the graphical confirmation of the mass fraction values, as indicated in Fig. 5. This enabled the determination of the fine content (<44 μm) with a resolution of 0.1 wt% on the graph depicted in Fig. 6.

Prior to employing the method for determining the size distribution of U_3Si_2 particles in the samples obtained following the scheme illustrated in Table 2, some preliminary studies were conducted. These studies aimed to ascertain the appropriate magnification level and the number of images to be utilized for this research. After the completion of these studies, the method for fine content determination was validated, thereby establishing its suitability for application in this fragmentation study. The outcomes of these preliminary investigations are presented and discussed in the subsequent sections.

2.3. Selection of magnification

The accuracy of digitally representing an object is influenced by image magnification, which refers to the resolution of the image. Choosing the appropriate image magnification is crucial to ensure optimal particle separation and resolution. Selecting the optimal magnification involves finding a balance between particle size and shape. Particle shape plays a role in accuracy due to the presence of jaggedness along the particle boundary, which can affect perimeter definition. For instance, accurately representing the perimeter of an elongated particle is more challenging compared to a square particle,

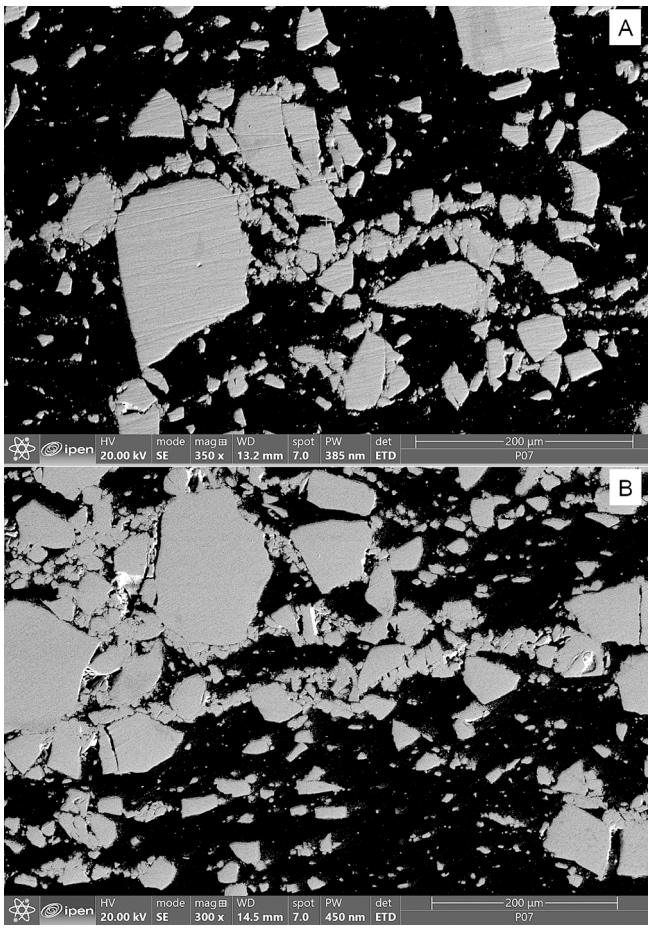

Fig. 3. Scanning electron micrographs (secondary electron images) of the longitudinal section in the rolling direction, enabling clear visualization of the fragmentation of the U_3Si_2 particles as well as the stringering phenomenon after the seventh rolling pass.

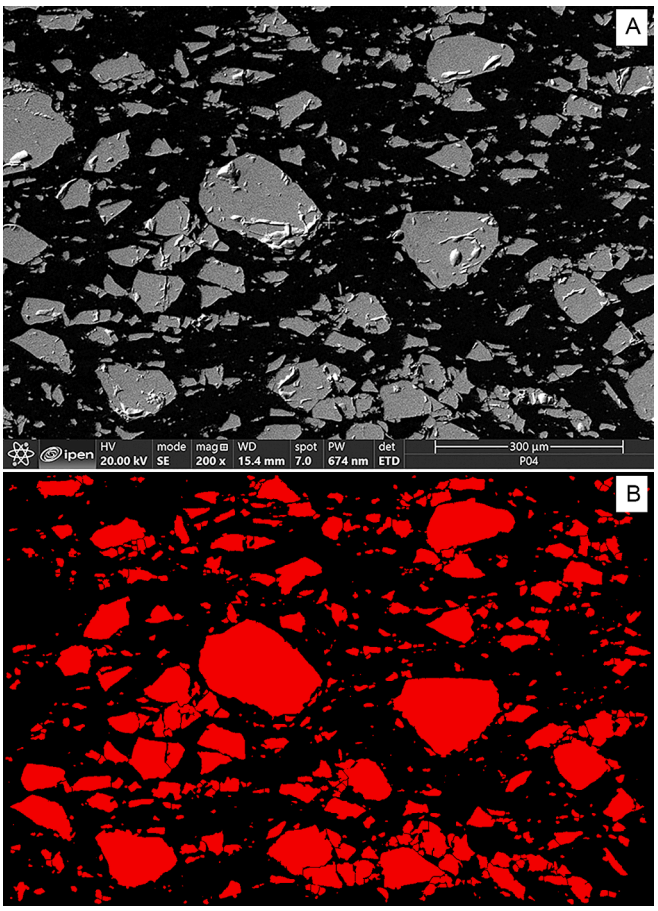

Fig. 4. Example of image processing utilized for the measurement of U_3Si_2 particle sizes through image analysis. (A) Represents the original image, while (B) illustrates the processed image.

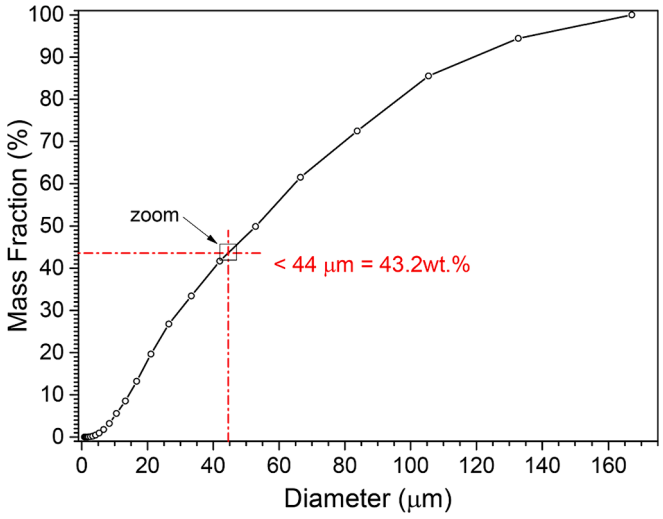

Fig. 5. Accumulated mass fraction curve derived from data extracted from images and processed using the Saltikov method.

leading to potentially reduced accuracy. Hence, low resolutions inevitably result in inaccuracies. Conversely, high resolutions necessitate a larger number of images to analyse an adequate quantity of particles.

A reference polished section of U_3Si_2 powder embedded in resin was utilized to test three different magnifications. The powder employed was identical to that used for the fabrication of the briquettes, comprising 20 wt% of fines (<44 µm). At 100X magnification, a resolution of 1.35 µm per pixel was achieved. The 200X magnification yielded a resolution of 0.67 µm, while the 300X magnification provided a resolution of 0.45 µm.

The magnification study involved measuring particle sizes in 10 images per magnification. The results of this study are visually presented in Fig. 7. The methodology utilized for determining the fine content (<44 µm) was as previously explained.

The three magnifications studied demonstrated a good approximation to the nominal value of the fines content (20 wt%) in the U_3Si_2 powder used in this study. Upon initial analysis, the 200X magnification provided the closest value to the nominal one. The 100X magnification yielded a slightly lower value, likely due to the underestimation of small particles resulting from the lower image resolution. On the other hand, the 300X magnification produced a slightly higher value, possibly because it disregarded large particles located at the image's border, which were not considered. This error is illustrated in Fig. 8. With higher magnification, there is an increased likelihood of large particles appearing at the image's border (Fig. 8A) and being excluded from the measurement (Fig. 8B).

2.4. Selection of the number of images

The accuracy of particle size determination using image analysis relies on measuring enough particles. To establish the minimum number required for a representative sample, ten images were progressively processed in a cumulative manner. This involved processing the first

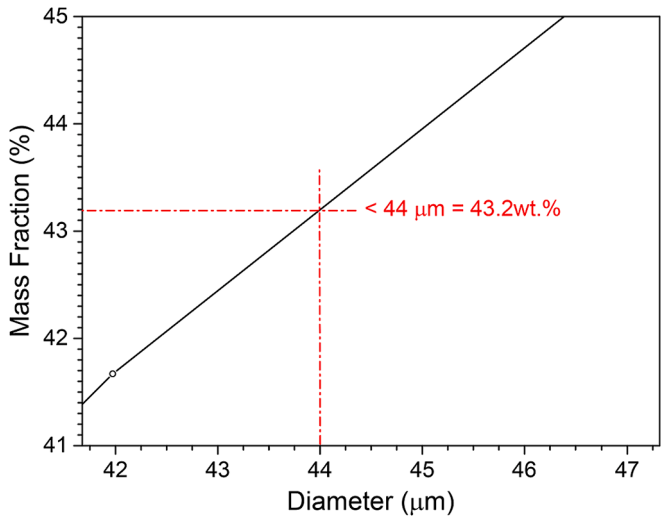

Fig. 6. Example of determining mass fraction values by directly reading from the graph. Values with a resolution of 0.1 wt% can be obtained.

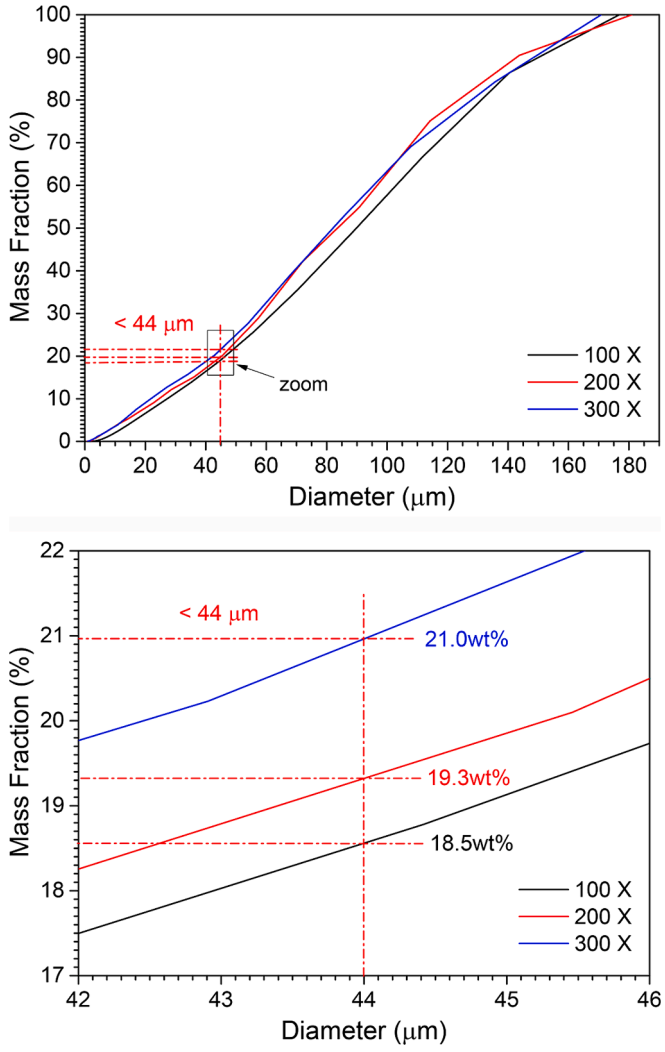

Fig. 7. Influence of magnification on the quantitative metallographic determination of fine content in the U_3Si_2 powder used in this study, with a nominal value of 20 wt% of fines below 44 μm.

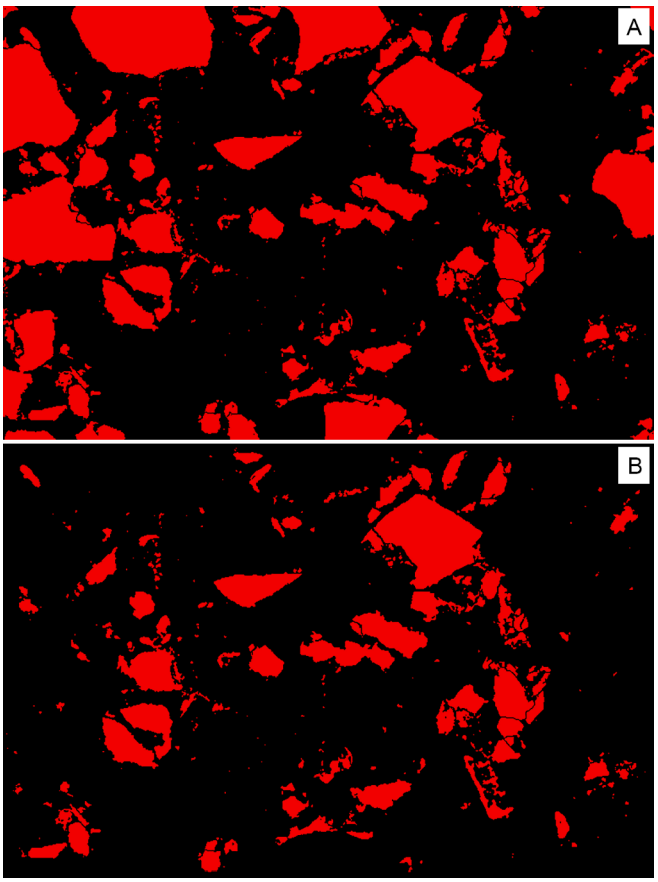

Fig. 8. Evidence of the influence of eliminating large particles at the edge of the image on the determination of fine content. The large particles at the image border (A) are excluded for the measurement (B).

image, collecting its data, and then incorporating the data from the second image into the accumulated dataset. The same process was repeated for subsequent images, with the accumulated data gradually expanding from one image to ten images. The outcomes of this analysis, conducted at the three magnifications studied, are depicted in Fig. 9. It was observed that after reaching a minimum number of processed images, the variation range of the fines value stabilizes within a specific range. These ranges for each of the studied magnifications are indicated in Fig. 9.

For the 100X magnification, even with just one processed image (1108 particles), the obtained result falls within the stabilization range. The fine content values range from 17.2 to 18.9 wt%, with a variation amplitude of 1.7 wt%.

For the 200X magnification, the fines content value falls within the variation range of 1.1 wt% after processing three images (1890 particles). All cumulative values up to the total of ten processed images fit within this range. In this case, the range is 18.9 to 20.0 wt%.

In the case of the 300X magnification, the stabilization of the fines content variation occurs after processing four images (1427 particles). The stabilization range varies from 20.1 to 21.3 wt%, with an amplitude of 1.2 wt%.

The results of this study demonstrate that processing five images is sufficient to obtain results within the indicated variation range shown in the graphs of Fig. 9. Additionally, the findings further support the recommendation of utilizing a magnification of 200X. Not only does it yield a value closer to the nominal fines content in the U_3Si_2 powder (20 wt%), but it also exhibits the smallest amplitude in the variation range when processing a minimum of three images. Therefore, based on these findings, it can be concluded that the 200X magnification is indeed the

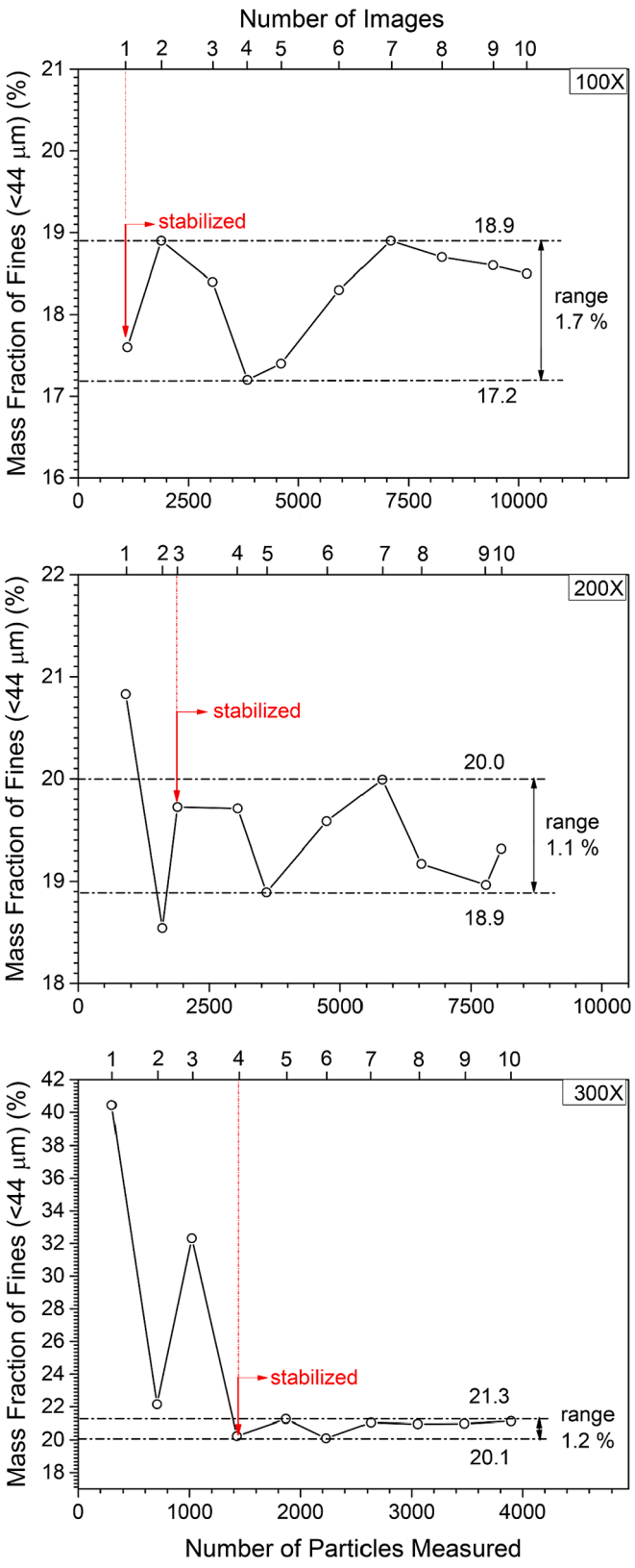

Fig. 9. The influence of the number of processed images on the results of the fine content (<44 µm) in U_3Si_2 powder for the three magnifications under study. The nominal value of fines in the U_3Si_2 powder is 20 wt%.

recommended choice. By processing five images, we can measure approximately 3500 particles.

Based on the presented results, this study has established the utilization of 200X magnification and the processing of five images as the chosen approach to determine the fine content, specifically particles smaller than 44 µm, within the fuel plate meat after each rolling pass.

2.5. Assessment of overall uncertainty

The findings depicted in Fig. 9 demonstrate that, for each individual sample, the image analysis method employed in this study allows for the estimation of the true fines content within a variation range of ± 1.1 wt %. To assess the overall uncertainty of the method, four U_3Si_2 powder samples were chosen from the batch manufactured at IPEN-CNEN/SP, with a measured fines content of < 44 µm at 20 wt%. These samples were prepared using metallography techniques, such as resin embedding and polishing.

For each powder sample, a total of five images were captured, and the particle size distribution was analyzed using image analysis. The method earlier explained was utilized to determine the fraction below 44 µm. The results are presented in Fig. 10.

The overall variation range among the four samples, as indicated in Fig. 10, was found to be 4.5 wt%, taking into account the internal variation estimated at 1.1 wt% for each sample. Consequently, the overall uncertainty of the method can be estimated to be ± 2.3 wt%. This level of uncertainty was deemed acceptable and satisfactory for the objectives of this study.

The average fines content value derived from the analysis of the four examined samples was determined to be 19.7 wt%. Consequently, there was a deviation of 0.3 wt% below the measured fines content present in the U_3Si_2 powder (reference). This deviation represents a 1.5 % deviation from the true value. In terms of accuracy, this level of deviation was deemed acceptable, considering the objectives of the current study.

3. Results and discussion

Fig. 11 illustrates the progression of fines content (<44 µm) in the fuel meat throughout the fuel plate rolling process. To validate the methodology employed in this study, like the approach used for U_3Si_2 powder, a cumulative evaluation of ten images from the final fuel plate's meat (after rolling pass 11) was conducted. The results of this analysis are presented in Fig. 12. It is evident that after processing five images, the fines value's variation stabilizes within a narrow range of ± 1.6 wt %. The comprehensive uncertainty of the method for the fuel plate

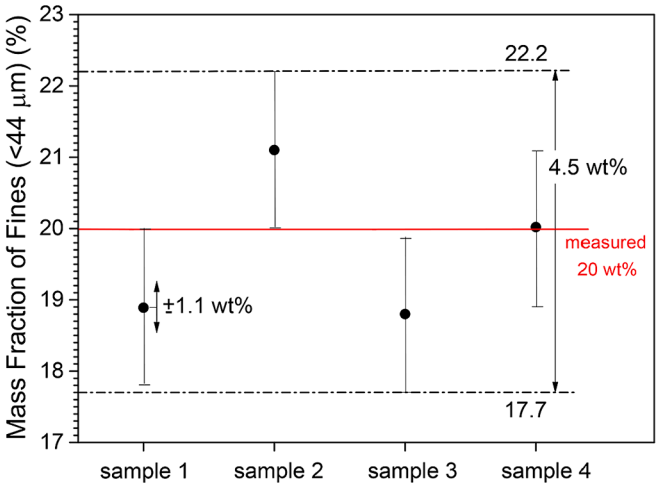

Fig. 10. Assessment of method variability for determining fines content using quantitative metallography.

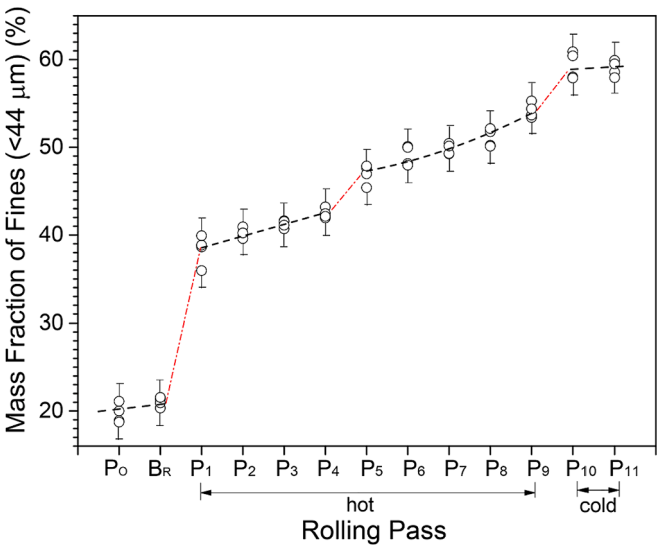

Fig. 11. Progression of U_3Si_2 fine content during fuel plate rolling.

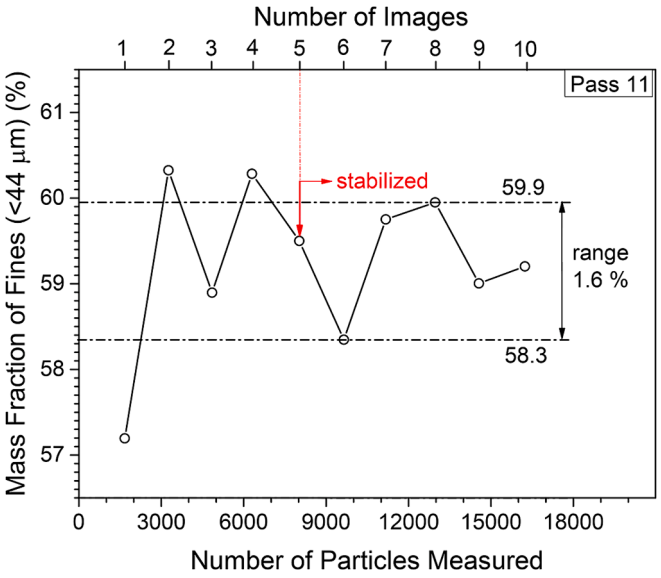

Fig. 12. Influence of the number of processed images on the results of the fine (<44 μm) content determination in the finished fuel plate meat (after rolling pass 11).

(across four samples) is depicted in Fig. 13. For each sample extracted following rolling pass 11, five images were captured and subjected to analysis.

Following rolling pass 11, an overall variation range of 5.1 wt% among the four samples, as depicted in Fig. 13, was observed. This range encompasses the internal variation, estimated at 1.6 wt% for each sample (Fig. 12). Thus, the comprehensive uncertainty of the method can be approximated at ± 2.5 wt%. The method's uncertainty level has increased from ± 2.3 wt%, as applied to U_3Si_2 powder, to ± 2.5 wt% when extended to the fuel plate meat post-fabrication (rolling pass 11). This potential elevation in uncertainty might stem from the heightened variability in fines content across the four samples, arising from the non-uniform U_3Si_2 particle fragmentation during rolling within the fuel plate meat. Despite this variability, it is deemed acceptable and adequate for the study's objectives. This level of uncertainty is indicated in Fig. 11.

To validate the accuracy of the methodology for high fines content, four U_3Si_2 powder samples containing 60 wt% fines (<44 μm) were

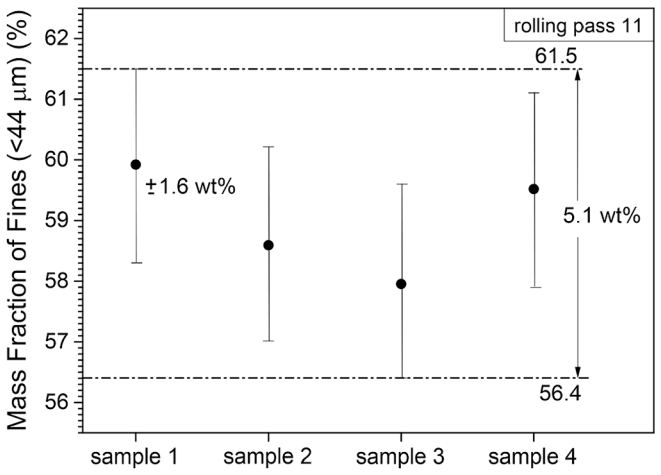

Fig. 13. Variability of the method for determining fines content after plate fabrication.

prepared using metallography techniques, involving resin embedding and polishing. The fines content determination methodology was then applied, and the resulting fines content values were presented in Table 3. The maximum observed deviation was 0.8 wt% above the nominal fine content present in the U_3Si_2 powder (reference). This outcome underscores the accuracy of the applied methodology, even when employed in the context of fuel plate meats, where the fine content is substantially higher (approximately 60 wt%) compared to the original powder's fines content (20 wt%).

In Fig. 11, a significant increase in the fines content becomes evident right from the initial hot rolling pass, surging from the initial 20 wt% found in the powder and briquette to surpass 38 wt% following the first rolling phase. This increase is attributed to the fragmentation of U_3Si_2 particles. Throughout the entirety of the hot rolling procedure, the fines content progressively rises with each rolling iteration. However, this increment does not follow a perfectly linear behavior; there's a subtle trend toward heightened fragmentation during the latter stages of hot rolling, specifically in rolling pass 5. This might be attributed to the reduction in the fuel meat's thickness during rolling, intensifying the interaction among U_3Si_2 particles and subsequently enhancing fragmentation. Possibly in rolling pass 5 the meat thickness reaches a critical value that results in an abrupt increase in fragmentation, thus increasing the fines content. This can best be seen in Fig. 14 (the meat thickness axis is on a logarithmic scale to better separate the points).

It's evident that fragmentation doesn't take place during the briquette pressing process, thereby maintaining the initial fines content of the U_3Si_2 powder. Nevertheless, in Fig. 15, there is clear evidence of cracking and partial disaggregation of U_3Si_2 particles during the pressing stage. In such instances, the cracked particles, as well as fragments from partially disaggregated particles (highlighted by arrows in Fig. 15), are not treated as separate entities. This interpretation accounts for the consistent fines content observed in both the briquette and the original powder.

The abrupt break in the curve depicted in Fig. 11 between passes 9 and 10 is elucidated by the shift from hot rolling to cold rolling. As evident from the figure, upon transitioning to cold rolling, the fines

Table 3
Assessment of method accuracy in the context of high fines content.

Sample	Measured Fine Content (wt%)	Deviation from the Nominal Fine content (wt%)
1	59.8	− 0.2
2	60.2	+ 0.2
3	60.8	+ 0.8
4	60.5	+ 0.5

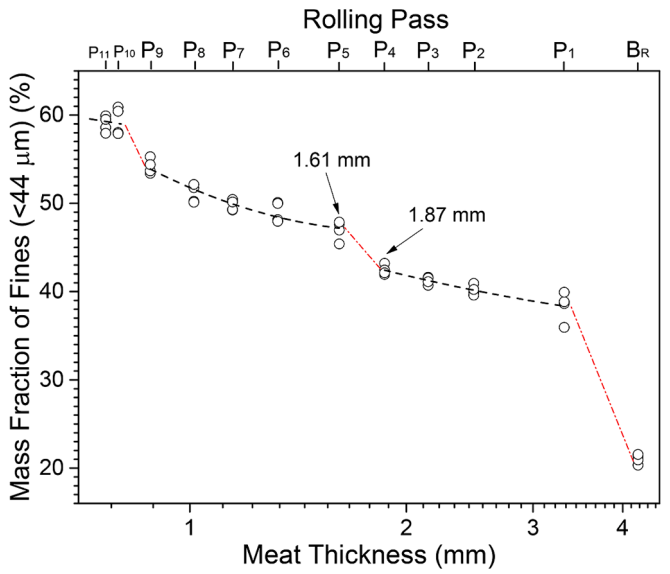

Fig. 14. Evolution of U_3Si_2 fine content with the meat thickness during fuel plate rolling.

content of the fuel plate meat increases notably. It is important to note that the reduction during cold rolling is merely half of that during the final hot passes. This signifies that the observed increase in fines content is not solely attributable to the rolling reduction but also to the shift from hot to cold rolling. During hot rolling, the elevated temperature of the aluminum matrix reduces its strength and increases its ductility, making it more deformable. In contrast, cold rolling occurs at room temperature, causing the aluminum matrix to become stronger. This increased strength, coupled with the deformation stresses induced by cold rolling, trigger substantial fragmentation of the U_3Si_2 particles. This fragmentation, in turn, leads to the observed increase in fines content.

During the transition from hot rolling to cold rolling, specifically between passes 9 and 10, there is a notable escalation in the prevalence of the stringering phenomenon. This observation is qualitative in nature since quantifying stringering proves challenging. A pioneering study investigating fragmentation in U_3O_8-Al dispersions executed manual quantification of stringering (Hobson and Leitten Jr, 1967). Fig. 16 serves as an attempt to illustrate the contrasting intensity of stringering between hot rolling (Pass 9) and cold rolling (Pass 10). In Pass 9, although stringering is present, it appears to be shorter and encompass larger particles (Fig. 16A), whereas in Pass 10, the stringering is more elongated, featuring smaller particles (Fig. 16B).

Fig. 17 provides a comparison between the initial size distribution of representative U_3Si_2 particles in the powder and the characteristic size distribution after the completion of the rolling process. The cumulative curves were formed using data collected from the four samples, comprising a total of 20 images. The intense fragmentation of U_3Si_2 particles during rolling is clearly evident in this figure. The influence of rolling on particle size distribution is substantial, causing a pronounced shift of the cumulative curve towards smaller dimensions. Notably, the fraction of U_3Si_2 particles below 44 µm nearly triples (from 20 wt% to 59.9 wt%), a trend evident in both Figs. 11 and 17.

It is important to highlight that the fines content within fuel meats is generally prone to underestimation. This limitation arises from the inherent challenge of image processing to effectively discern small agglomerated U_3Si_2 particles, particularly those found in stringering phenomena. The small particles in the stringering were not well discriminated, as show in Fig. 18. Following image processing, the fine U_3Si_2 particles are not entirely separated, as seen in Fig. 18B. This discrepancy becomes apparent when comparing this processed image with the original depiction in Fig. 18A. Clusters of extremely fine

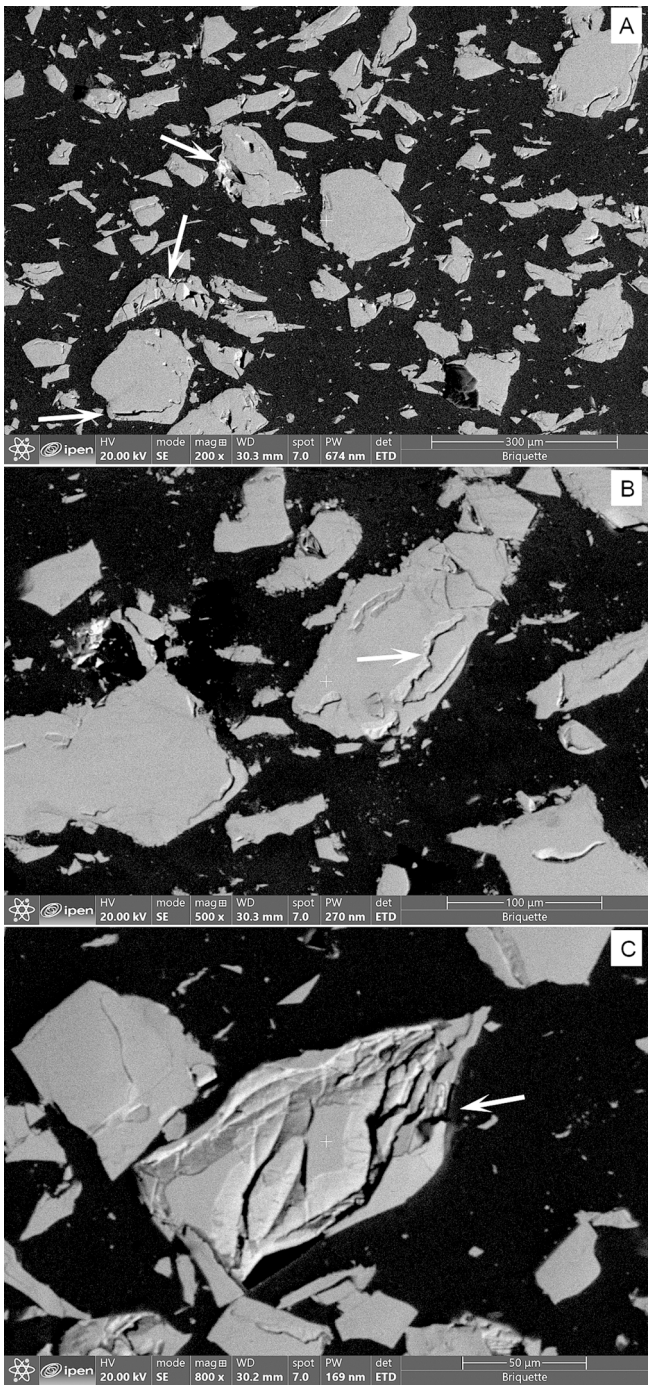

Fig. 15. Scanning electron micrographs (secondary electron images) showing cracking (B) and partial disaggregation (C) of U_3Si_2 particles after briquette pressing.

particles are treated as individual entities post image processing. While it's challenging to precisely quantify the extent of underestimation in the values presented in Fig. 11, an approximate estimate could be 1 wt%, accounting for the deviation observed in the case of the reference sample containing 60 wt% of fines < 44 µm.

Fragmentation of fuel particles during the rolling process of dispersions is a well-documented phenomenon. Back in the 1960s, Hobson and Leitten Jr. (1967) conducted a study on U_3O_8-Al dispersions investigating particle fragmentation. This phenomenon is likely to occur in any system where the fuel particles are friable. An illustrative scheme depicting particle fragmentation during the production of dispersion-

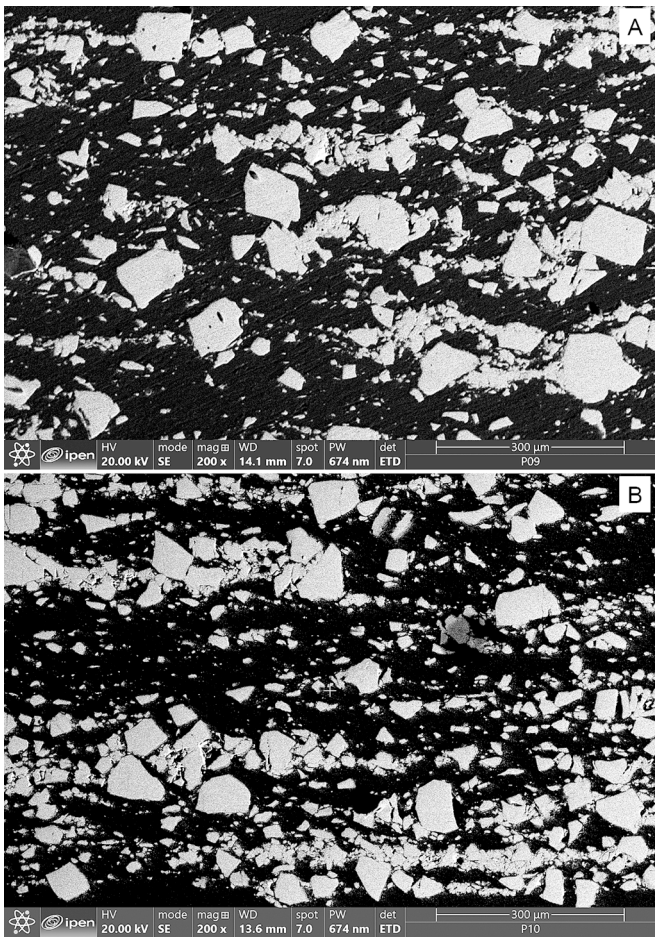

Fig. 16. Comparative scanning electron micrographs (secondary electron images) depicting stringering phenomena between Pass 9 (final hot rolling pass) and Pass 10 (initial cold rolling pass). Image (A) illustrates stringering during Pass 9, while image (B) displays the stringering observed in Pass 10.

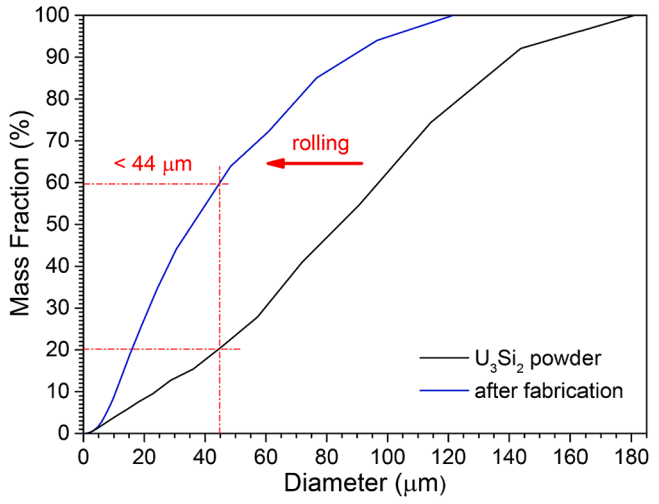

Fig. 17. Influence of rolling on U_3Si_2 particle size distribution.

based fuels was provided by Hobson and Leitten Jr. (1967), and it has been adapted in Fig. 19 for reference.

Fig. 20 presents an overview of the results acquired during the fuel plate rolling process. This compilation integrates data sourced from the four samples, comprising a total of 20 images.

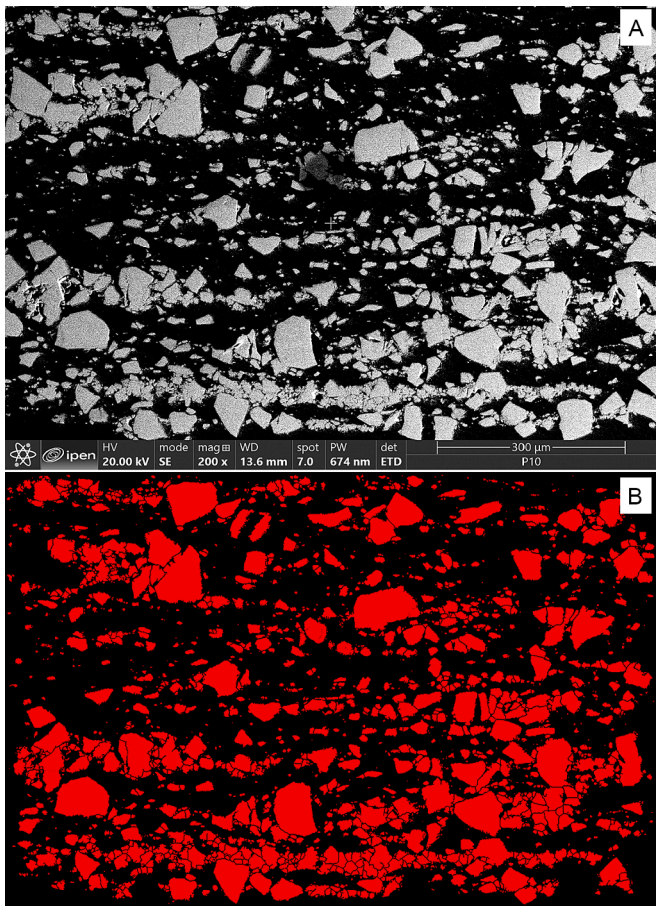

Fig. 18. Evidence of underestimation of U_3Si_2 fine particles agglomerated in stringering.

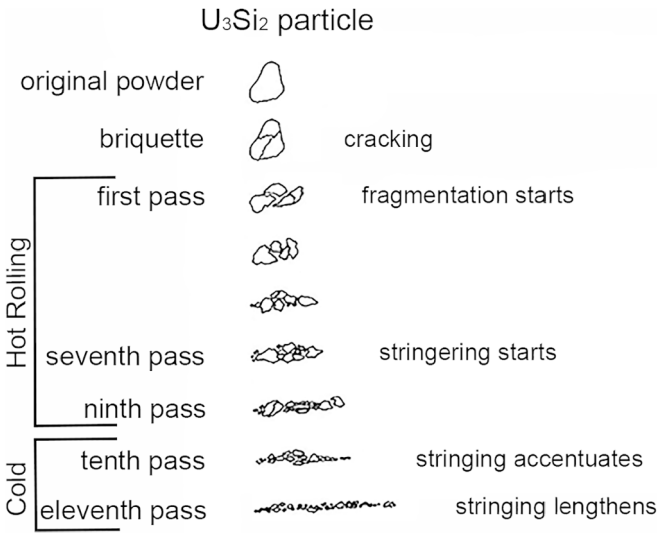

Fig. 19. Representation of the evolution of the fragmentation of a U_3Si_2 particle during rolling the fuel plate.
Adapted from Hobson and Leitten Jr. (1967)

Therefore, a new specification for U_3Si_2 powder, containing 30 wt% of particles smaller than 44 µm (fines), is not expected to significantly alter the U_3Si_2 particle size distribution after the manufacture of the fuel plate. Additional work is underway to experimentally verify this finding.

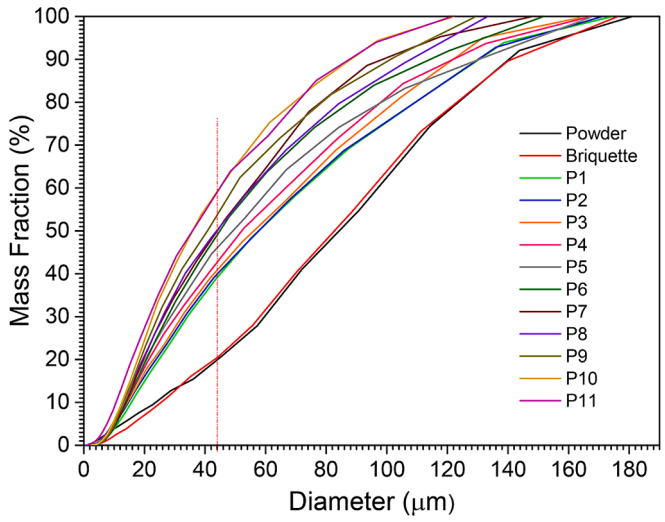

Fig. 20. Cumulative curves depicting the particle size distribution at each stage of fuel plate fabrication through rolling.

4. Conclusions

The findings of this work demonstrate that the content of particles smaller than 44 μm (referred to as fines) originally present in the U_3Si_2 powder is substantially increased during the manufacture of the fuel plate by rolling. The value increased from 20 wt% to 59 wt%. Therefore, the specification of the maximum fines content in the U_3Si_2 powder is not effective for ensuring good quality of the dispersion in the meat of the fuel plate. Rather than solely specifying the fines content in the powder, it becomes more significant to define the maximum allowable fines content within the meat of the final fuel plate.

The results also indicate that increasing the fines content (<44 μm) in the U_3Si_2 powder from 20 to 30 wt% will not significantly alter the fines content in the meat of the finished fuel plate. This would allow for the use of all U_3Si_2 powder produced, eliminating the need for recycling during the manufacturing process. However, this proposal will still need to be demonstrated, experimentally verifying if these changes will not increase the fines content present in the meat of the fuel plate currently manufactured at IPEN. Work with this goal is in progress.

It is important to note that the results obtained are valid only for the IPEN-CNEN/SP manufacturing conditions, since the fragmentation and stringering of U_3Si_2 particles during rolling depends on the volumetric fraction of U_3Si_2 in the fuel meat, the rolling conditions, and the characteristics of the U_3Si_2 powder, such as density and morphology. While plate fabrication shows a marked tendency to produce fines, each manufacturer has its own particle fragmentation phenomena. The use of ductile uranium compounds such as UMo, which have high resistance to fragmentation, are likely not to be subject to stringering and will maintain the original fines content in the powder unchanged during the manufacture of the fuel plate, which would allow for better control of the fuel meat microstructure, bringing it closer to an ideal dispersion. Work is underway to prove this assumption.

CRediT authorship contribution statement

Michelangelo Durazzo: Conceptualization, Data curation, Formal analysis, Investigation, Methodology, Project administration, Supervision, Writing – original draft. **Gilberto Hage Marcondes:** Investigation, Data curation. **Elita Fontenele Urano de Carvalho:** Visualization, Investigation. **Guilherme Duarte de Barros:** Investigation, Data curation. **Ricardo Mendes Leal Neto:** Validation, Methodology, Investigation, Formal analysis, Writing – review & editing.

Declaration of competing interest

The authors declare that they have no known competing financial interests or personal relationships that could have appeared to influence the work reported in this paper.

Data availability

Data will be made available on request.

Acknowledgments

The authors are grateful to the National Council for Scientific and Technological Development (CNPq) for the research grants 407438/2023-8, 304034/2015-0, 310274/2012-5 and 470363/2012-6 provided for this work.

References

Abdelrazek, I.D., Moursy, S.M., Zidan, W. I., 1999, Specifications, production and inspection procedures of the fuel element produced by the Egyptian fuel manufacturing pilot plant. In: International symposium on research reactor utilization, safety and management, Lisbon, Portugal, 6-10 Sep 1999. IAEA-SM–360/52P (available at: https://inis.iaea.org/collection/NCLCollectionStore/_Public/30/044/30044480.pdf?r=1).

Adelfang, P., Alvarez, L., Boero, N., Calabrese, R., Echenique, P., Markiewicz, M., Pasqualini, E., Ruggirello, G., Taboada, H., 2002. Advances and highlights of the CNEA qualification program as high density fuel manufacturer for research reactors. available at 6 International Topical Meeting on Research Reactor Fuel Management, Ghent, Belgium.

Copeland, G.L., Hobbs, R.W., Hofman, G.L., Snelgrove, J.L., 1987, Performance of low-enriched U_3Si_2-Al dispersion fuel elements in the Oak Ridge Research Reactor. Argonne National Laboratory, Argonne, Illinois, October 1987. ANL/RERTR/TM-10 (available at https://doi.org/10.2172/5560545).

Cunningham, J.E., Boyle, E.J., 1955, MTR-Type fuel elements. International Conference on Peaceful Uses of Atomic Energy. Geneva, 8-20 August, V. 9, 1955, pp. 203-7.

Durazzo, M., Riella, H.G., 2015. 2015, Procedures for manufacturing nuclear research reactor fuel elements. OmniScriptum GmbH & Co. KG, Saarbrücken, Germany.

Durazzo, M., Urano de Carvalho, E.F., Saliba Silva, A.M., Souza, J.A.B., Riella, H.G., 2007. Current status of U_3Si_2 fuel elements fabrication in Brazil. available at International Meeting on Reduced Enrichment for Research and Test Reactors, Prague, Czech republic.

Durazzo, M., Vieira, E., Urano de Carvalho, E.F., Riella, H.G., 2017a. Evolution of fuel plate parameters during deformation in rolling. J. Nucl. Mater. 490, 197–210. https://doi.org/10.1016/j.jnucmat.2017.04.018.

Durazzo, M., Saliba-Silva, A.M., Martins, I.C., Urano de Carvalho, E.F., Riella, H.G., 2017b. Manufacturing low enriched uranium metal by magnesiothermic reduction of UF_4. Ann. Nucl. Energy 110, 874–885. https://doi.org/10.1016/j.anucene.2017.07.033.

Hobson, D.O., Leitten Jr., C.F., 1967, Characterization of U_3O_8 dispersions in aluminum. Oak Ridge National Laboratory, Oak Ridge, Tennessee, 1967. ORNL-TM-1692 (available at https://doi.org/10.2172/4452516).

Kaufman, A.R., 1962. Nuclear reactor fuel elements, metallurgy and fabrication. Interscience, New York, N.Y., p. 1962

Perrotta, J.A., Soares, A.J., 2014. RMB: The new Brazilian Multipurpose Research Reactor. In: International Topical Meeting on Research Reactor Fuel Management RRFM 2014, Ljubljana, Slovenia, 20 March – 3 April, P. 394-401, 2014 (available at: https://www.euronuclear.org/download/proceedings-rrfm-2014/).

Saltikov, S.A., 1967. The Determination of the size distribution of particles in an opaque material from a measurement of the size distribution of their sections. Stereology 163–173. https://doi.org/10.1007/978-3-642-88260-9_31.

Suripto, A., Supardjo, A.S., Sardjono, D.I., 1995, Development of high loading fuel at BATAN. In: 18 international meeting on Reduced Enrichment for Research and Test Reactors, Paris, France, 17-21 Sep 1995. (available at https://inis.iaea.org/collection/NCLCollectionStore/_Public/35/044/35044398.pdf?r=1.

Weber, C.E., 1959. Progress in dispersion elements. Series V Progress in Nuclear Energy. Metalurgy and Fuels. Pergamon Press.

Weber, C.E., Hirsch, H.H., 1955, Dispersion-Type fuel elements. In: International Conference on Peaceful Uses of Atomic Energy. Geneva, 8-20 August, V. 9, 1955, pp. 196-202.

Weber, C.E., Hirsch, H.H., 1956. Dispersion type fuel elements. Series V Progress in Nuclear Energy. Metalurgy and Fuels. Pergamon Press.

White, D.W., Beard, A P., Willis A H., 1957, Irradiation behavior of dispersion fuels. Knolls Atomic Power Laboratory, Schenectady, New York. United States Atomic Energy Commission, 1957. KAPL-1909 (available at https://www.osti.gov/servlets/purl/4317012).